frontiers in Energy Research

ORIGINAL RESEARCH
published: 23 June 2021
doi: 10.3389/fenrg.2021.710626

Transient Thermal Analysis of a Solar-Assisted AHU by Focusing on Heat Recovery and Nanoparticles: Jeddah Climate Zone

Yacine Khetib [1,2]*

[1]Mechanical Engineering Department, Faculty of Engineering, King Abdulaziz University, Jeddah, Saudi Arabia, [2]Center Excellence of Renewable Energy and Power, King Abdulaziz University, Jeddah, Saudi Arabia

In the Jeddah climate region, a lot of energy is assigned to the air handling unit (AHU) sector, which should be reduced by using energy-efficient solutions. As the air passes through the cooling coil, a lot of energy is consumed to reduce the temperature along with humidity so that if the air is precooled in the previous stages, energy consumption in this energy-intensive section will be diminished. Using the coldness of the return air in the heat recovery unit (HRU), the incoming air is precooled. Based on the thermodynamic calculations, in June, July, and August, the cooling coil power demand reduces by 11.6, 13.3, and 12%, respectively. In summer, owing to using HRU, an energy-saving by 76.08 MWh is achieved (12.34% reduction in energy demand). By the incorporation of the solar collectors in the AHU, heating coil demand diminishes by 1,206, 1,399, and 1,367 kWh in June, July, and August, respectively. To improve the solar-assisted AHU effectiveness, the MWCNT nanoparticles are injected into the collectors, and it is found that the saving-energy capability improves by 17.7% using MWCNT-water at 0.1 vol.%.

Keywords: air handling unit, solar collector, energy-saving, nanofluid, heat recovery

OPEN ACCESS

Edited by:
Mohsen Sharifpur, University of Pretoria, South Africa

Reviewed by:
Houman Yarmand, Delft University of Technology, Netherlands
Cong Qi, China University of Mining and Technology, China

***Correspondence:**
Yacine Khetib
ykhetib@yahoo.com
ykhateb@kau.edu.sa

Specialty section:
This article was submitted to Process and Energy Systems Engineering, a section of the journal Frontiers in Energy Research

Received: *16 May 2021*
Accepted: *26 May 2021*
Published: *23 June 2021*

Citation:
Khetib Y (2021) Transient Thermal Analysis of a Solar-Assisted AHU by Focusing on Heat Recovery and Nanoparticles: Jeddah Climate Zone. Front. Energy Res. 9:710626. doi: 10.3389/fenrg.2021.710626

INTRODUCTION

Residential buildings, along with commercial buildings, are heavily involved in CO_2 emission and energy demand. Buildings consume 40% of energy consumption (EIA, 2019) while accounting for about 35% of CO_2 emission. To reduce the energy demand along with CO_2 emission, it is recommended to focus on the intensive-energy sector (Jokar et al., 2017; Ahmadi et al., 2019; Attia et al., 2020; Hashemi-Tilehnoee et al., 2020; Jamei et al., 2021; Thalib et al., 2021), one of which is the air handling unit (AHU). To reduce the energy demand, many researchers focused on recovery-based approaches (Noussan et al., 2017; Eades, 2018; Pacak et al., 2019; Dodoo, 2020; Liu et al., 2020; ShahsavarGoldanlou et al., 2020).

Almitani et al. (2021) added an energy recovery unit (ERU) to the AHU to reduce the use of energy. In their attractive design, the exhaust air energy is used to preheat the fresh air. Fresh air

Abbreviations: $c_{p,wf}$, working fluid specific heat; ERU, energy recovery unit; E_{Amb}, ambient air energy content; E_{room}, room air energy content; HRU, heat recovery unit; I_c, Solar intensity over collector; $\dot{m}_{fresh}$, fresh air mass fraction; $\dot{m}_{wf}$, working fluid mass flow rate; P_c, collector heat gain; PC_{AHU}, AHU power consumption ; PC_{CC}, cooling coil power consumption; PC_{HC}, heating coil power consumption; SHWS, Solar hot water supply; T_{outlet}, collector outlet temperature; T_{inlet}, collector inlet temperature; T_{set}, storage tank setpoint; T_{Amb}, ambient temperature; T_{room}, room temperature; ϕ_{room}, room relative humidity; ϕ_{Amb}, ambient humidity; η_c, collector efficiency; η_{AHU}, AHU efficiency.

passes through ERU, absorbs the sensible/latent energy of the exhaust air, and therefore, its energy rises. When the outside air is very cold, there is a risk of frostbite, so it is necessary to preheat the fresh air by installing an auxiliary heater. Hence, first, the fresh air is preheated and then enters ERU. Through recovery energy, energy demand in various devices reduces. Due to recovery of sensible/latent energies in ERU (owing to exchanging temperature and humidity), the heater and humidifier energy demand reduce. Due to the temperature growth in ERU, the auxiliary heater was able to raise the air temperature by consuming less energy (up to 37.4%). Humidifier also increases humidity by consuming less steam (up to 61.2%). Because, the fresh air humidity is increased by passing through ERU by passing through ERU. Reducing energy demand in these sectors reduced the total AHU power load by 31.8% and increased efficiency (η_{AHU}) by 46.6%. Also, the authors considered the exergy destruction in AHU and revealed that installing ERU decreased irreversibility from 82.54 to 55.33 kW. Therefore, another positive point of ERU can be considered as a reduction in exergy losses by 33%.

Kalbasi et al. (2020a), through developing a program in EES software, examined the sensitivity of ERU to the extent of humidity in ambient. They added an ERU to the AHU and considered different scenarios. In the first scenario, they increased ϕ_{Amb} from 30 to 70% (T_{Amb} = cte) and found that energy recovery augmented by 234%. They also considered the variations of the cooling coil energy-consuming (PC_{cc}). Taking into account the reduction in PC_{cc} by 13.63% at ϕ_{Amb} = 30% and by 27.7% at ϕ_{Amb} = 70%, it is concluded that ERU effectiveness is more in a humid region. They also examined the effects of T_{Amb}. At ϕ_{Amb} = 50%, as T_{Amb} rises from 30 to 40°C, PC_{cc} intensifies by 122 kW which is equivalent to a 38.18% intensification in PC_{cc}. The variation in PC_{cc} effects η_{AHU} and decreases it by 23.56%. Note that the sensitivity of PC_{cc} to T_{Amb} depends on the ambient relative humidity (ϕ_{Amb}). As ϕ_{Amb} rises, PC_{cc} and η_{AHU} become more sensitive to T_{Amb}. The authors examined the total energy recovery in ERU. At 30°C and 30%, ERU could recover the energy by 42.6 kW while at 40°C and 70%, this figure was 300 kW. This indicates that ERU in humid and hot climates has more efficacy.

In another study (Kalbasi et al., 2020b) the authors studied the exergy performance of an AHU + ERU. The major irreversibility corresponded to the heating coil (11.47 kW) while the minimum irreversibility (1.067 kW) was through the mixing box. Owing to using ERU, irreversibility diminished by 2.87 kWh. This is very acceptable because an 8.7-percent reduction in irreversibility improves the second efficiency by 4.6%.

In a numerical/experimental study, Ribé et al. (2019) examined the effects of relative humidity on the performance of ERU. Since in the heat recovery unit (HRU), only the sensible heat is exchanged; therefore, the humidity content does not affect the HRU effectiveness. The latent heat transfer potential of the ERU unit depends on ϕ_{Amb}. Although in dry climates, they showed that there was not much difference between ERU and HRU, but for wet climates, the amount of recovered energy in ERU is higher. Taking into account the Spanish climatic zone, they recommended using HRU in the dry climate (owing to lower cost) and ERU in the wet climate.

In a similar study, Yari et al. (2019) examined the effects of ϕ_{Amb} on the usefulness of adding ERU in AHU. In dry climate ϕ_{Amb} = 10%, PC_{cc} reduced only by 0.161 kW (0.9%) while in the wet climate, PC_{cc} diminished by 10 kW (27%). Moreover, the efficiency was influenced by ϕ_{Amb} so that at ϕ_{Amb} = 10%, installing ERU improved η_{AHU} by 1% while at ϕ_{Amb} = 70% this figure was 36.8%. Therefore in humid climates the usefulness of ERU becomes more evident.

Zheng et al. (2020) added two ERUs in an AHU and focused on PC_{AHU}. Under the Kuwait city climate, the thermodynamic analysis showed that PC_{AHU} for AHU without the ERU unit is 438.74 kW while after incorporating two ERUs in AHU, PC_{AHU} reduces by 163.63 kW. This means that PC_{AHU} diminished owing to installing ERUs by 37.3%.

Controllers with the apparent commands can reduce PC_{AHU}. In a study by Homod (2014), it was revealed that PC_{AHU} experiences a 32-percent reduction if control scheduling is optimized. The results of other studies in the field of energy consumption reduction are reported.

In this study, two strategies are used to reduce AHU energy consumption (PC_{AHU}). In the first strategy, by reducing the fresh air temperature through using HRU, PC_{CC} diminishes. In the second strategy, a solar collector is used to reduce PC_{HC}. This collector, which is filled with MWCNT nanoparticles, can provide a part of the required energy for the heating coil and thus improve the overall performance of AHU. Finally, the amount of energy-saving in each scenario is compared.

DESCRIPTION OF THE MODIFIED AHU

The description of the solar system integrated with AHU is shown in **Figure 1**. In general, AHUs have two main purposes: 1—providing the suitable temperature (T_{room}) along with the apparent relative humidity (ϕ_{room}), 2—providing fresh air ($\dot{m}_{fresh}$) to satisfy comfort conditions.

As shown in **Figure 1**, the ambient fresh air enters the AHU with the thermodynamic properties of T_{Amb} and ϕ_{Amb} (**Figure 2**). The average of T_{Amb} in June is 31.5°C while in July and August it is 33.5°C. The average of ϕ_{Amb} is 56.6, 51.2, and 58.3% in June, July, and August, respectively.

If the task of the AHU is only to supply $\dot{m}_{fresh}$, it can be said that the AHU needs a fan and duct to transfer fresh air, and therefore PC_{AHU} will be insignificant. There is always a big difference between T_{Amb} and T_{room} along with ϕ_{Amb} and ϕ_{room} and hence the energy content of the indoor (E_{room}) and outdoor (E_{Amb}). Taking into account $E_{Amb} > E_{room}$ in summer, the AHU should dissipate the effects of Q_s and Q_s through the cooling and heating coils. For meeting the ventilation requirements, $\dot{m}_{fresh}$ and supply air mass flow rate ($\dot{m}_{supply}$) should be justified as follows:

$$\dot{m}_{fresh} = \frac{N \times 0.006}{\vartheta}, \quad (1)$$

$$\dot{m}_{supply} = \frac{n \times \forall}{3600 \times \vartheta}, \quad (2)$$

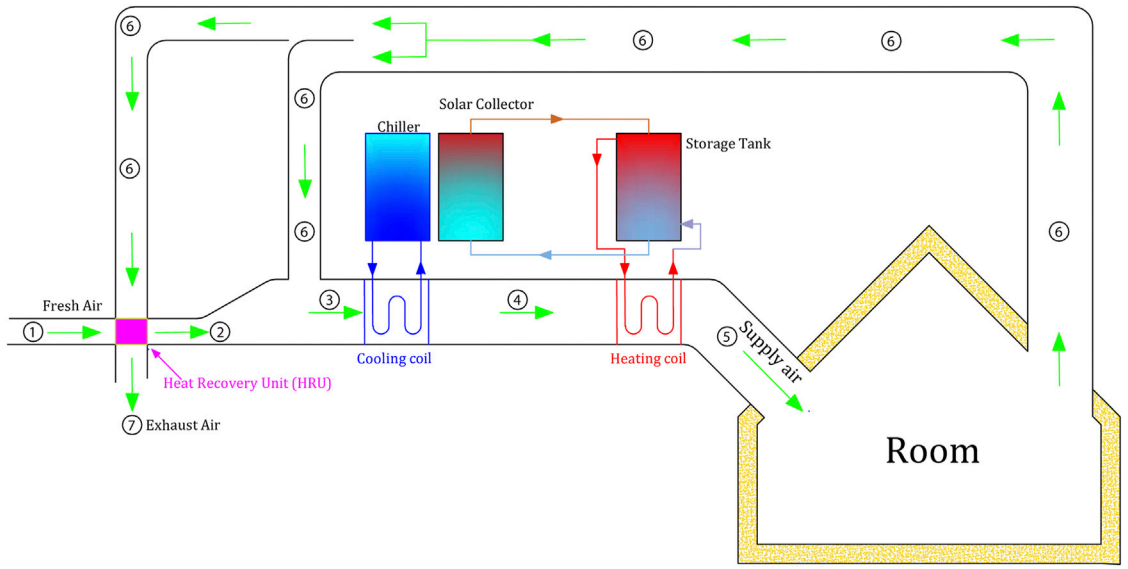

FIGURE 1 | Solar-assisted AHU.

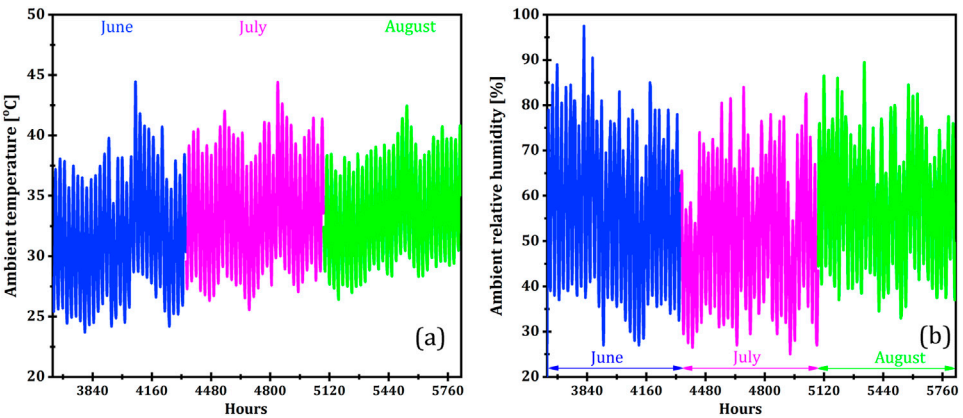

FIGURE 2 | Ambient properties (Jeddah, 21.48°N, 39.19°E).

where N is the number of people, 0.006 m^3/s is the fresh air mass flow rate per person, ϑ is the specific volume, $n = 6$ is the number of changes of air per hour, and $\forall$ denotes the room volume. First, air enters HRU. The absolute temperature and humidity of the air at the outlet are determined according to the following equation:

$$\begin{aligned} Q_{\mathrm{HRU}} &= \varepsilon_{\mathrm{HRU}}\, \dot{m}_{\mathrm{fresh}} c_p\, (T_1 - T_6), \\ T_2 &= T_1 - \frac{Q_{\mathrm{HRU}}}{\dot{m}_{\mathrm{fresh}} c_p}, \\ \omega_2 &= \omega_1, \\ T_7 &= T_6 + \frac{Q_{\mathrm{HRU}}}{\dot{m}_{\mathrm{fresh}} c_p}, \\ \omega_7 &= \omega_6, \end{aligned} \tag{3}$$

where $\varepsilon_{\mathrm{HRU}}$ is the effectiveness of the HRU unit. Note that in this study a transient analysis is performed for an AHU. In the transient analysis, there are changes in energy within the system so that its value depends on $\partial T/\partial t$. However, if the time step is selected small enough, the temperature changes within each control volume can be considered negligible ($(\partial T/\partial t) \rightarrow 0$). In this study, the same technique (assuming a small time step) is used. After that, the precooled air enters the mixing box. The outlet properties are (Kalbasi et al., 2020c):

$$h_3 = \frac{\dot{m}_2 h_2 + \left(\dot{m}_{\mathrm{supply}} - \dot{m}_{\mathrm{fresh}}\right) h_6}{\dot{m}_2 + \left(\dot{m}_{\mathrm{supply}} - \dot{m}_{\mathrm{fresh}}\right)}, \tag{4}$$

$$\omega_3 = \frac{\dot{m}_2 \omega_2 + \left(\dot{m}_{\mathrm{supply}} - \dot{m}_{\mathrm{fresh}}\right) \omega_6}{\dot{m}_2 + \left(\dot{m}_{\mathrm{supply}} - \dot{m}_{\mathrm{fresh}}\right)}. \tag{5}$$

After mixing, the air enters CC. After leaving CC, the properties are determined as follows:

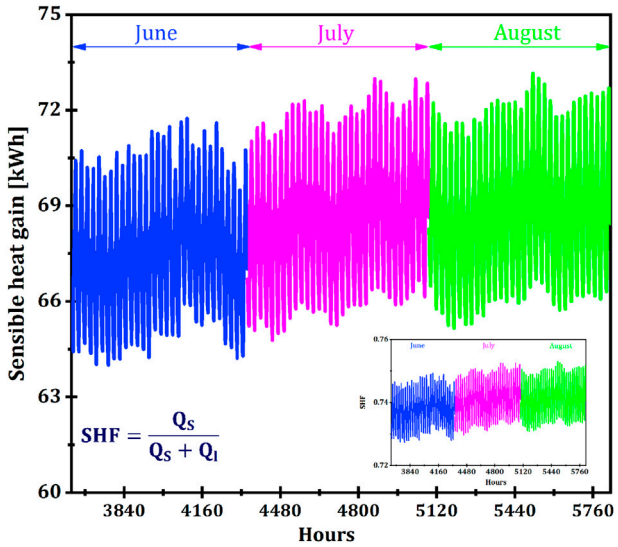

FIGURE 3 | The variations of Q_s and SHF parameters.

$$h_4 = \mathrm{BF}(h_3 - h_{\mathrm{ADP}}) + h_{\mathrm{ADP}}, \quad (6)$$

$$\omega_4 = \mathrm{BF}(\omega_3 - \omega_{\mathrm{ADP}}) + \omega_{\mathrm{ADP}}. \quad (7)$$

Because through passing CC, both humidity and temperature decrease, so $\mathrm{PC_{CC}}$ is obtained from the following equation:

$$\mathrm{PC_{CC}} = \underbrace{\dot{m}_{\mathrm{supply}} c_p (T_3 - T_4)}_{\text{sensible}} + \underbrace{\dot{m}_{\mathrm{supply}} h_{fg} (\omega_3 - \omega_4)}_{\text{latent}}. \quad (8)$$

The conditions for the supply air depend on $\underbrace{Q_s}_{\text{sensible}}$ and $\underbrace{Q_l}_{\text{latent}}$ and obtained from the following equations:

$$T_5 = T_6 - \frac{Q_s}{\dot{m}_{\mathrm{supply}} c_p}, \quad (9)$$

$$\omega_5 = \omega_6 - \frac{Q_l}{\dot{m}_{\mathrm{supply}} h_{fg}}. \quad (10)$$

Equations 9 and **10** reveal that the supply air properties are influenced by Q_s and Q_l. In air conditioner calculations, the parameter of SHF = $Q_s/(Q_s + Q_l)$ is usually used. The variations in Q_s along with SHF are shown in **Figure 3**.

$$\mathrm{PC_{HC}} = \dot{m}_{\mathrm{supply}} c_p (T_5 - T_4). \quad (11)$$

In this study, using a solar hot water supply (SHWS), the heating coil power demand ($\mathrm{PC_{HC}}$) is supplied. The solar system consists of three main parts: collectors, storage tank, and auxiliary heater. In the storage tank, the water must be set at a certain temperature (T_{set}). For this purpose, if the power of the collectors is not enough to regulate the temperature, the electric heater is turned on to adjust the temperature. The power of the collectors is obtained from the following equation:

$$P_c = \dot{m}_{wf} c_{p,wf} (T_{\mathrm{outlet}} - T_{\mathrm{inlet}}) = \eta_c \times I_c, \quad (12)$$

where $\dot{m}_{wf}$ is the working fluid mass flow rate. The parameters of η_c and I_c are collector efficiency and solar intensity. The variations in η_c and I_c are illustrated in **Figure 4** and **Figure 5**, respectively.

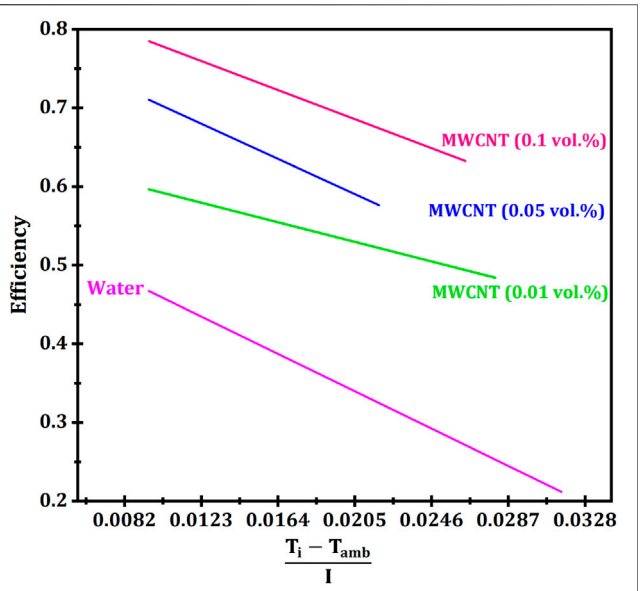

FIGURE 4 | The efficiency of the solar collector by using MWCNT nanoparticles (Eltaweel and Abdel-Rehim, 2019).

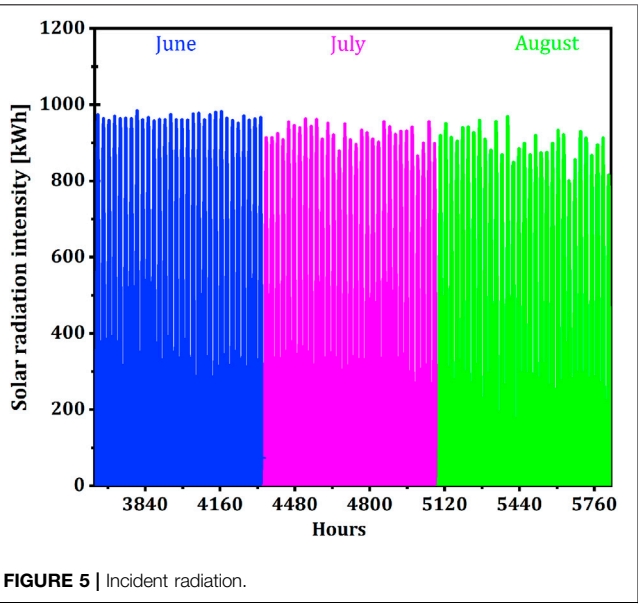

FIGURE 5 | Incident radiation.

RESULTS

In this study, it is tried to reduce $\mathrm{PC_{AHU}}$ in two scenarios. In the first scenario, the main focus is on reducing $\mathrm{PC_{CC}}$, while in the second scenario, the parameter of $\mathrm{PC_{CH}}$ is targeted.

FIRST SCENARIO

In summer, outdoor air energy (E_{Amb}) is at a higher level than the indoor one (E_{room}). To reduce $E_{\mathrm{Amb}} - E_{\mathrm{room}}$, a cooling coil should

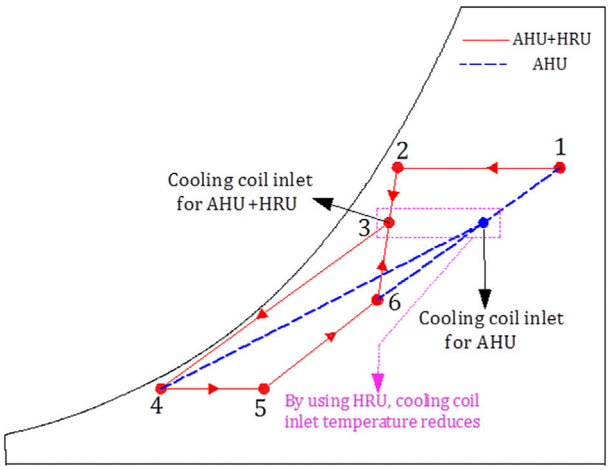

FIGURE 6 | Psychometric process of AHU and AHU + HRU.

be used. Finally, according to the ambient conditions shown in **Figure 2**, the ambient dew point is more than 6°C and therefore the air humidity along with temperature reduces through passing the cooling coil. By installing HRU, the temperature and humidity at the inlet of the cooling coil experience a reduction, and this means a reduction in PC_{CC}. As shown in **Figure 6**, the temperature of the air intake for AHU + HRU is lower than that in AHU.

Figure 7 illustrates the cooling coil power changes for AHU and AHU + HRU. It is clear that in June, the values of PC_{CC} are lower for AHU + HRU, and this trend is also true in July and August.

A lower PC_{CC} for AHU + HRU means energy-saving. The total amount of energy-saving in June, July, and August is 21.78, 27.2, and 27.1 MWh, respectively (**Figure 8**). In other words, cooling coil energy consumption reduces by 11.6, 13.3, and 12% in June, July, and August, respectively. Throughout the summer, PC_{cc} decreases by 12.34%, which resulted in a 76.09 MWh energy-saving.

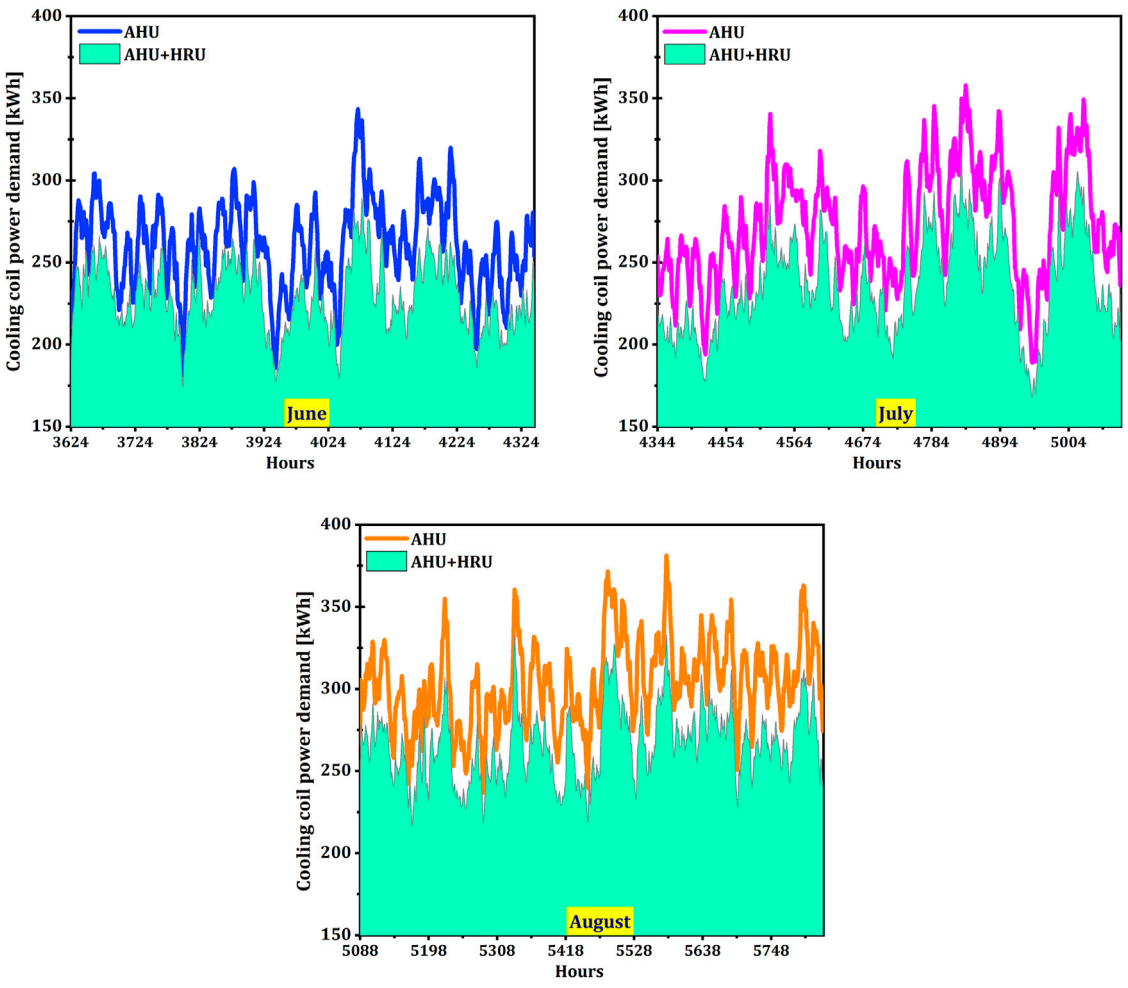

FIGURE 7 | PC_{CC} comparison between AHU and AHU + HRU.

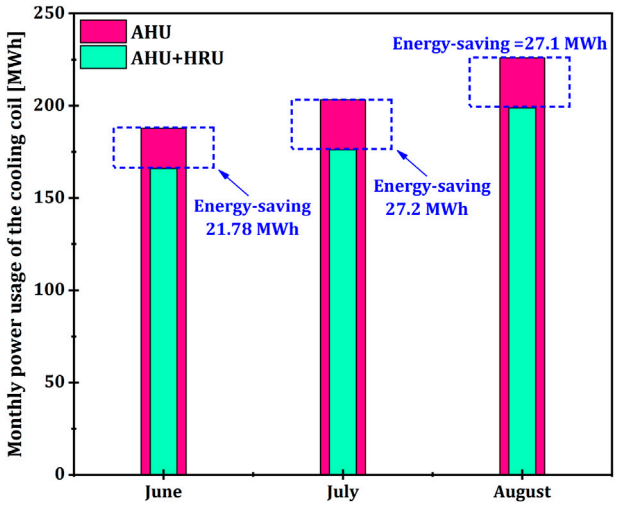

FIGURE 8 | The monthly power demand of the cooling coil.

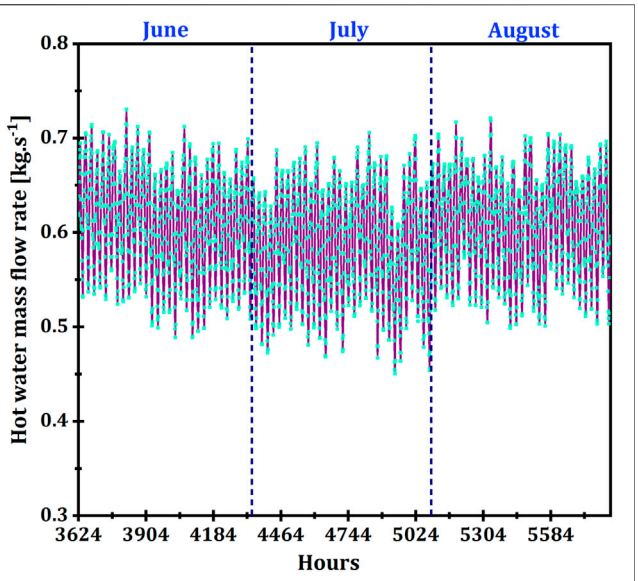

FIGURE 9 | Required hot water mass flow rate.

SECOND SCENARIO

In the second scenario, the focus is on the heating coil. Many studies showed the effectiveness of using solar energy (Ahmadi et al., 2017a; Ahmadi et al., 2017b; Ahmadi et al., 2018; Dabiri et al., 2018; Gholipour et al., 2020). In the heating coil, the temperature rises during a process in which the humidity ratio remains constant. The inlet temperature in the heating coil is preset according to the cooling coil outlet. On the other hand, the outlet temperature of the heating coil is also determined according to the room conditions using **Eq. 9**. Therefore, its input and output are predetermined. Generally, in AHUs, the heating coil supplies its energy through either a boiler or an electric heater. In this study, the heating coil power demand is supplied from a solar system. As mentioned in the previous section, the solar system consists of several collectors and a storage tank equipped with an electric heater. If solar energy cannot heat the water in the tank, the auxiliary heater must heat the water. In this study, in addition to the auxiliary heater, the tank is equipped with two sensors. The first sensor is located exactly at the top of the tank and the second sensor is located in the middle of the tank. The sensors function in such a way that they can keep the temperature in the whole tank in the range of 35–40°C. Since the power of the heating coil is obtained from $PC_{HC} = \dot{m}_{hotwater} \times 4180(\Delta T_{hotwater})$, so the parameters of $\dot{m}_{hotwater}$ and $\Delta T_{hotwater}$ are both known as independent variables. In air conditioning calculations, the selection of $\Delta T_{hotwater}$ and $\dot{m}_{hotwater}$ should be done in such a way that the difference between the inlet and outlet temperatures ($\Delta T_{hotwater}$) is equal to 20°F (ASHRAE American Society of Heating and Engineers, 2016). Therefore, taking into account $\Delta T_{hotwater} = 20$°F, the required hot water mass flow rate follows **Figure 9**. It is clear that the parameter of $\dot{m}_{hotwater}$ varies within the range of 0.4 – 0.8 kg/s.

Owing to the temperature range of 35 – 40 °C inside the storage tank, the heater power will change according to **Figure 10**. In this figure, the useful heat gain through the collector is also

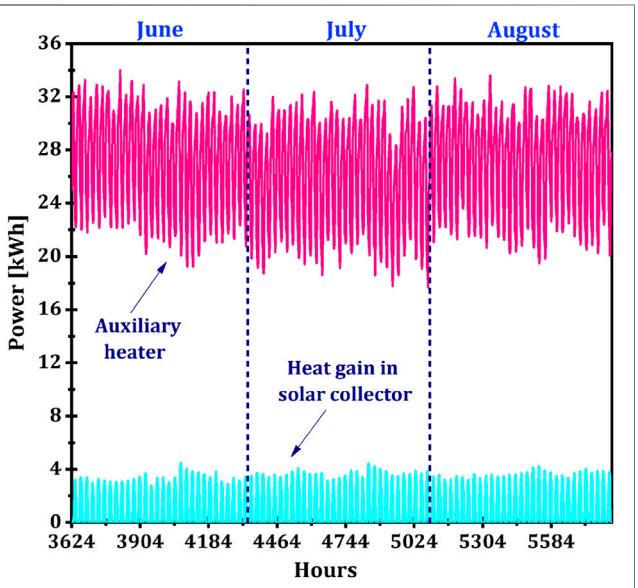

FIGURE 10 | Power usage in an auxiliary heater as well as power gain in a collector.

shown. This figure clearly shows that the heat gain in the collector is not enough to completely cover PC_{HC}.

For comparison, it is assumed that AHU provides heating power in the heating coil through an electric heater. Thermodynamic calculations affirm that accumulated heating power (PC_{HC}) in June, July, and August is 20.462, 20.303, and 21.142 MWh, respectively. However, by integrating AHU with a solar system, PC_{HC} can be reduced. **Figure 11** illustrates the monthly analysis of PC_{HC} and shows that it is less for the AHU + solar system.

Owing to integrating a solar system with AHU, PC_{HC} reduces by 0.85, 0.97, and 0.95 MWh in June, July, and August, respectively.

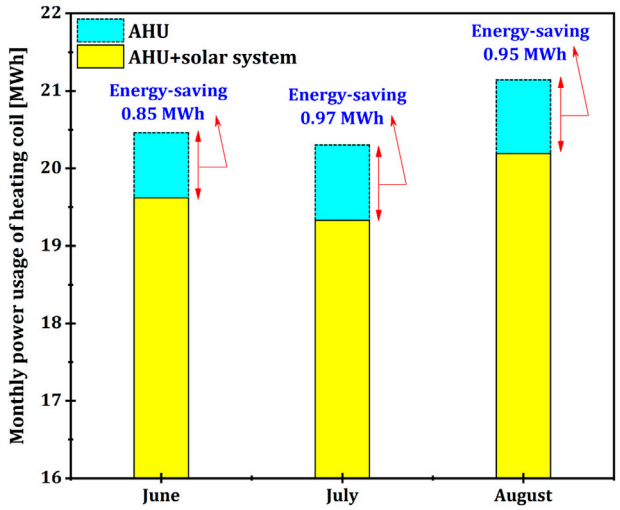

FIGURE 11 | The comparison of PC_{HC} between simple AHU and solar-assisted AHU.

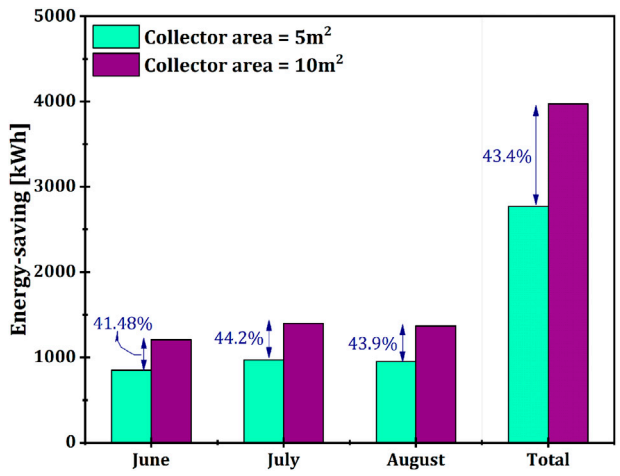

FIGURE 12 | Energy-saving in different months and dependency on collector area.

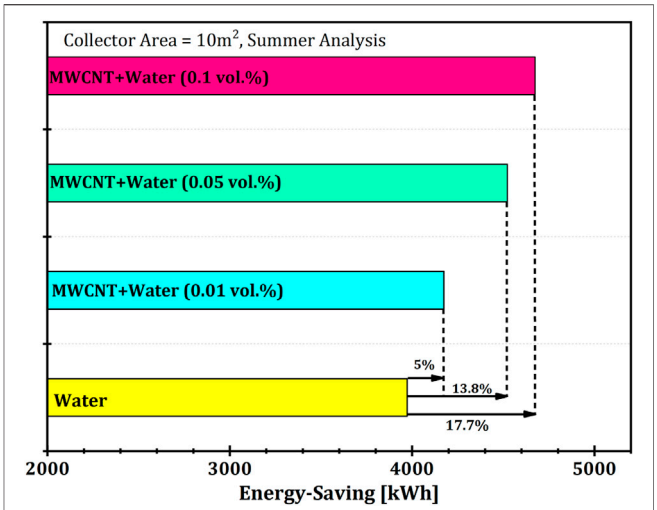

FIGURE 13 | Energy-saving increase owing to adding MWCNT/water in collectors.

It seems that by increasing the number of collectors in parallel arrangement (increasing the collector area), it is possible to strengthen the ability of energy-saving. As the area increases (as shown in **Figure 12**), the saving energy intensifies. In June, the saving energy increases by 41.48% (from 850 kWh to 1,206 kWh) as the area rises from 5 to 10 m^2. This figure for July and August is 44.22 and 43.9%. This implies that there is no linear relationship between the collector area and energy-saving content. Note that this figure in summer is 43.4% (with increasing area from 5 to 10 m^2).

Nanoparticles are another technique for improving the collectors' efficiency (Qu et al., 2019; Mahmoudi et al., 2020; Alawi et al., 2021; Sadeghi et al., 2021). These materials have widely been examined by many researchers (Osman et al., 2019; Yan et al., 2020; Aghakhani et al., 2020; Eshgarf et al., 2021; Mahdavi et al., 2020; Nguyen et al., 2020; Yan et al., 2020). Nanoparticles can improve heat transfer within the collector (Muhammad et al., 2016; Tong et al., 2019; Elcioglu et al., 2020; Yan et al., 2020; Gholipour et al., 2021; Mustafa et al., 2021). As shown in **Figure 5**, the efficiency for the MWCNT-based collector is higher. Therefore, it is expected that MWCNTs will increase the energy-saving content. In **Figure 13**, it can be seen that for a collector filled with water, the energy-saving is 3,972 kWh. This figure for collector filled with MWCNTs (at 0.01 vol.%) is 4,170 kWh. This indicates that using MWCNT is recommended owing to a 5% enhancement in energy-saving.

The positive effects of MWCNT increase as the nanoparticle concentration intensifies. Adding further MWCNTs leads to more enhancement in energy-saving. At 0.05 and 0.1 vol.%, the energy-saving is 4,520 and 4,675 kWh which is equivalent to 13.8 and 17.7% enhancement.

CONCLUSION

Considering the 40 and 35% contributions of the building sector in energy consumption and greenhouse gas emissions, two techniques were used to reduce both the parameters. In the first technique, a unit heat recovery (HRU) was used to reduce energy demand in the cooling coil, while in the second technique, the energy consumption in the heating coil was reduced by focusing on solar energy. By developing energy and continuity equations in individual sections, transient thermal analysis of the AHU was performed. The main results were:

❖ First technique (installing HRU):

1. By installing HRU, the hotness from the fresh air was transferred to the return air and consequently, the fresh air was precooled. Owing to entering with a lower temperature into the cooling coil, the power demand reduced by 76.09 MWh in summer which is equivalent to a 12.34% reduction.

❖ Second technique (using solar collectors + stratified storage tank):

1. In summer, the task of the heating coil is to adjust the thermodynamic conditions of the supply air. With the installation of the solar system, energy consumption was reduced by 3,972 kWh in June + July + August which is equivalent to a 6.41-percent reduction.
2. To boost the solar collector effectiveness, MWCNT nanoparticles were loaded into the water and it was found that the energy-saving potential increased by 17.7% (from 3,972 to 4,675 kWh).

DATA AVAILABILITY STATEMENT

The original contributions presented in the study are included in the article/Supplementary Material, further inquiries can be directed to the corresponding author.

AUTHOR CONTRIBUTIONS

YK: Writing, Methodology, Software.

FUNDING

This project was funded by the Deanship of Scientific Research (DSR) at King Abdulaziz University, Jeddah, under Grant Nos. (135-007-D1433).

ACKNOWLEDGMENTS

The author, therefore, acknowledge with thanks DSR technical and financial support.

REFERENCES

Aghakhani, S., Pordanjani, A. H., Afrand, M., Sharifpur, M., and Meyer, J. P. (2020). Natural Convective Heat Transfer and Entropy Generation of Alumina/water Nanofluid in a Tilted Enclosure with an Elliptic Constant Temperature: Applying Magnetic Field and Radiation Effects. *Int. J. Mech. Sci.* 174, 105470. doi:10.1016/j.ijmecsci.2020.105470

Ahmadi, G., Toghraie, D., and Akbari, O. A. (2017). Efficiency Improvement of a Steam Power Plant through Solar Repowering. *Ijex* 22 (2), 158–182. doi:10.1504/ijex.2017.083015

Ahmadi, G., Toghraie, D., and Akbari, O. A. (2017). Solar Parallel Feed Water Heating Repowering of a Steam Power Plant: A Case Study in Iran. *Renew. Sustain. Energ. Rev.* 77, 474–485. doi:10.1016/j.rser.2017.04.019

Ahmadi, G., Toghraie, D., and Akbari, O. A. (2018). Technical and Environmental Analysis of Repowering the Existing CHP System in a Petrochemical Plant: A Case Study. *Energy* 159, 937–949. doi:10.1016/j.energy.2018.06.208

Ahmadi, M. H., Alhuyi Nazari, M., Sadeghzadeh, M., Pourfayaz, F., Ghazvini, M., Ming, T., et al. (2019). Thermodynamic and Economic Analysis of Performance Evaluation of All the thermal Power Plants: A Review. *Energy Sci Eng* 7 (1), 30–65. doi:10.1002/ese3.223

Alawi, O. A., Kamar, H. M., Mallah, A. R., Mohammed, H. A., Kazi, S. N., Che Sidik, N. A., et al. (2021). Nanofluids for Flat Plate Solar Collectors: Fundamentals and Applications. *J. Clean. Prod.* 291, 125725. doi:10.1016/j.jclepro.2020.125725

Almitani, K. H., Abu-Hamdeh, N. H., Golmohammadzadeh, A., and Javaheran Yazd, M. (2021). The Effect of Various Forms of the Tube Cross on the Energetic and Exergetic Analysis of Helical Tube in Tube Heat Exchangers of an AHU with Energy Recovery Unit in Heating Mode: Injection of Vapor/water Particles. *J. Therm. Anal. Calorim.* doi:10.1007/s10973-020-10546-9

ASHRAE American Society of Heating, R., and Engineers, A-C. (2016). *ASHRAE handbook-HVAC Systems and Equipment*. IP Edition. Georgia: ASHRAE.

Attia, M. E. H., Karthick, A., Manokar, A. M., Driss, Z., Sathyamurthy, R., and Sharifpur, M. (2020). Sustainable Potable Water Production from Conventional Solar Still during the winter Season at Algerian Dry Areas: Energy and Exergy Analysis. *J. Therm. Anal. Calorim.*, 1–11.

Dabiri, S., Khodabandeh, E., Poorfar, A. K., Mashayekhi, R., Toghraie, D., and Abadian Zade, S. A. (2018). Parametric Investigation of thermal Characteristic in Trapezoidal Cavity Receiver for a Linear Fresnel Solar Collector Concentrator. *Energy* 153, 17–26. doi:10.1016/j.energy.2018.04.025

Dodoo, A. (2020). Primary Energy and Economic Implications of Ventilation Heat Recovery for a Multi-Family Building in a Nordic Climate. *J. Building Eng.* 31, 101391. doi:10.1016/j.jobe.2020.101391

Eades, W. G. (2018). Energy and Water Recovery Using Air-Handling Unit Condensate from Laboratory HVAC Systems. *Sustain. Cities Soc.* 42, 162–175. doi:10.1016/j.scs.2018.07.006

EIA, U. (2019). *International Energy Outlook 2019: With Projections to 2050* Washington, DC: Office of Energy Analysis.

Elcioglu, E. B., Genc, A. M., Karadeniz, Z. H., Ezan, M. A., and Turgut, A. (2020). Nanofluid Figure-Of-Merits to Assess thermal Efficiency of a Flat Plate Solar Collector. *Energ. Convers. Manag.* 204, 112292. doi:10.1016/j.enconman.2019.112292

Eltaweel, M., and Abdel-Rehim, A. A. (2019). Energy and Exergy Analysis of a Thermosiphon and Forced-Circulation Flat-Plate Solar Collector Using MWCNT/Water Nanofluid. *Case Stud. Therm. Eng.* 14, 100416. doi:10.1016/j.csite.2019.100416

Eshgarf, H., Kalbasi, R., Maleki, A., and Shadloo, M. S. (2021). A Review on the Properties, Preparation, Models and Stability of Hybrid Nanofluids to Optimize Energy Consumption. *J. Thermal Anal. Calorim.* 144 (5), 1959–1983.

Gholipour, S., Afrand, M., and Kalbasi, R. (2020). Improving the Efficiency of Vacuum Tube Collectors Using New Absorbent Tubes Arrangement: Introducing Helical Coil and Spiral Tube Adsorbent Tubes. *Renewable Energy* 151, 772–781.

Gholipour, S., Afrand, M., and Kalbasi, R. (2021). Introducing Two Scenarios to Enhance the Vacuum U-Tube Solar Collector Efficiency by Considering Economic Criterion. *J. Taiwan Inst. Chem. Eng.* doi:10.1016/j.jtice.2021.04.015

Hashemi-Tilehnoee, M., Dogonchi, A. S., Seyyedi, S. M., and Sharifpur, M. (2020). Magneto-fluid Dynamic and Second Law Analysis in a Hot Porous Cavity Filled by Nanofluid and Nano-Encapsulated Phase Change Material Suspension with Different Layout of Cooling Channels. *J. Energ. Storage* 31, 101720. doi:10.1016/j.est.2020.101720

Homod, R. Z. (2014). Assessment Regarding Energy Saving and Decoupling for Different AHU (Air Handling Unit) and Control Strategies in the Hot-Humid Climatic Region of Iraq. *Energy* 74, 762–774. doi:10.1016/j.energy.2014.07.047

Jamei, M., Ahmadianfar, I., Olumegbon, I. A., Asadi, A., Karbasi, M., Said, Z., et al. (2021). On the Specific Heat Capacity Estimation of Metal Oxide-Based Nanofluid for Energy Perspective - A Comprehensive Assessment of Data Analysis Techniques. *Int. Commun. Heat Mass Transfer* 123, 105217. doi:10.1016/j.icheatmasstransfer.2021.105217

Jokar, M. A., Ahmadi, M. H., Sharifpur, M., Meyer, J. P., Pourfayaz, F., and Ming, T. (2017). Thermodynamic Evaluation and Multi-Objective Optimization of Molten Carbonate Fuel Cell-Supercritical CO 2 Brayton Cycle Hybrid System. *Energ. Convers. Manag.* 153, 538–556. doi:10.1016/j.enconman.2017.10.027

Kalbasi, R., Ruhani, B., and Rostami, S. (2020a). Energetic Analysis of an Air Handling Unit Combined with Enthalpy Air-To-Air Heat Exchanger. *J. Therm. Anal. Calorim.* 139 (4), 2881–2890. doi:10.1007/s10973-019-09158-9

Kalbasi, R., Izadi, F., and Talebizadehsardari, P. (2020b). Improving Performance of AHU Using Exhaust Air Potential by Applying Exergy Analysis. *J. Therm. Anal. Calorim.* 139 (4), 2913–2923. doi:10.1007/s10973-019-09198-1

Kalbasi, R., Shahsavar, A., and Afrand, M. (2020c). Reducing AHU Energy Consumption by a New Layout of Using Heat Recovery Units. *J. Therm. Anal. Calorim.* 139 (4), 2811–2820. doi:10.1007/s10973-019-09070-2

Liu, W., Kalbasi, R., and Afrand, M. (2020). Solutions for Enhancement of Energy and Exergy Efficiencies in Air Handling Units. *J. Clean. Prod.* 257, 120565. doi:10.1016/j.jclepro.2020.120565

Mahdavi, M., Sharifpur, M., Meyer, J. P., and Chen, L. (2020). Thermal Analysis of a Nanofluid Free Jet Impingement on a Rotating Disk Using Volume of Fluid in Combination with Discrete Modelling. *Int. J. Therm. Sci.* 158, 106532. doi:10.1016/j.ijthermalsci.2020.106532

Mahmoudi, A., Fazli, M., Morad, M. R., and Gholamalizadeh, E. (2020). Thermo-hydraulic Performance Enhancement of Nanofluid-Based Linear Solar Receiver Tubes with Forward Perforated Ring Steps and Triangular Cross Section; a Numerical Investigation. *Appl. Therm. Eng.* 169, 114909. doi:10.1016/j.applthermaleng.2020.114909

Muhammad, M. J., Muhammad, I. A., Che Sidik, N. A., and Muhammad Yazid, M. N. A. W., "Thermal Performance Enhancement of Flat-Plate and Evacuated Tube Solar Collectors Using Nanofluid: A Review," *Int. Commun. Heat Mass Transfer,* vol. 76, pp. 6–15. (2016). doi:10.1016/j.icheatmasstransfer.2016.05.009

Mustafa, J., Alqaed, S., and Kalbasi, R. (2021). Challenging of Using CuO Nanoparticles in a Flat Plate Solar Collector- Energy Saving in a Solar-Assisted Hot Process Stream. *J. Taiwan Inst. Chem. Eng.* doi:10.1016/j.jtice.2021.04.003

Nguyen, Q., Bahrami, D., Kalbasi, R., and Karimipour, A. (2020). Functionalized Multi-Walled Carbon Nano Tubes Nanoparticles Dispersed in Water through an Magneto Hydro Dynamic Nonsmooth Duct Equipped with Sinusoidal-wavy wall: Diminishing Vortex Intensity via Nonlinear Navier-Stokes Equations. *Math. Meth Appl. Sci.*. doi:10.1002/mma.6528

Noussan, M., Carioni, G., Degiorgis, L., Jarre, M., and Tronville, P. (2017). Operational Performance of an Air Handling Unit: Insights from a Data Analysis. *Energ. Proced.* 134, 386–393. doi:10.1016/j.egypro.2017.09.579

Osman, S., Sharifpur, M., and Meyer, J. P. (2019). Experimental Investigation of Convection Heat Transfer in the Transition Flow Regime of Aluminium Oxide-Water Nanofluids in a Rectangular Channel. *Int. J. Heat Mass Transfer* 133, 895–902. doi:10.1016/j.ijheatmasstransfer.2018.12.169

Pacak, A., Jedlikowski, A., Karpuk, M., and Anisimov, S. (2019). Analysis of Power Demand Calculation for Freeze Prevention Methods of Counter-flow Heat Exchangers Used in Energy Recovery from Exhaust Air. *Int. J. Heat Mass Transfer* 133, 842–860. doi:10.1016/j.ijheatmasstransfer.2018.12.144

Qu, J., Zhang, R., Wang, Z., and Wang, Q. (2019). Photo-thermal Conversion Properties of Hybrid CuO-Mwcnt/h2o Nanofluids for Direct Solar thermal Energy Harvest. *Appl. Therm. Eng.* 147, 390–398. doi:10.1016/j.applthermaleng.2018.10.094

Ribé, O., Ruiz, R., Quera, M., and Cadafalch, J. (2019). Analysis of the Sensible and Total Ventilation Energy Recovery Potential in Different Climate Conditions. Application to the Spanish Case. *Appl. Therm. Eng.* 149, 854–861. doi:10.1016/j.applthermaleng.2018.12.076

Sadeghi, G., Pisello, A. L., Nazari, S., Jowzi, M., and Shama, F. (2021). Empirical Data-Driven Multi-Layer Perceptron and Radial Basis Function Techniques in Predicting the Performance of Nanofluid-Based Modified Tubular Solar Collectors. *J. Clean. Prod.* 295, 126409. doi:10.1016/j.jclepro.2021.126409

Shahsavar Goldanlou, A., Kalbasi, R., and Afrand, M. (2020). Energy Usage Reduction in an Air Handling Unit by Incorporating Two Heat Recovery Units. *J. Building Eng.* 32, 101545. doi:10.1016/j.jobe.2020.101545

Thalib, M. M., Vimala, M., Manokar, A. M., Sathyamurthy, R., Sadeghzadeh, M., and Sharifpur, M. (2021). Energy, Exergy and Economic Investigation of Passive and Active Inclined Solar Still: Experimental Study. *J. Therm. Anal. Calorim.*, 1–12.

Tong, Y., Lee, H., Kang, W., and Cho, H., "Energy and Exergy Comparison of a Flat-Plate Solar Collector Using Water, Al2O3 Nanofluid, and CuO Nanofluid," *Appl. Therm. Eng.,* vol. 159, p. 113959, (2019). doi:10.1016/j.applthermaleng.2019.113959

U.S. Energy Information Administration (). Available at: https://www.eia.gov/totalenergy/data/monthly/2021.

Yan, S.-R., Golzar, A., Sharifpur, M., Meyer, J. P., Liu, D.-H., and Afrand, M. (2020). Effect of U-Shaped Absorber Tube on thermal-hydraulic Performance and Efficiency of Two-Fluid Parabolic Solar Collector Containing Two-phase Hybrid Non-newtonian Nanofluids. *Int. J. Mech. Sci.* 185, 105832. doi:10.1016/j.ijmecsci.2020.105832

Yan, S.-R., Kalbasi, R., Nguyen, Q., and Karimipour, A. (2020). Sensitivity of Adhesive and Cohesive Intermolecular Forces to the Incorporation of MWCNTs into Liquid Paraffin: Experimental Study and Modeling of Surface Tension. *J. Mol. Liq.*, 113235.

Yari, M., Kalbasi, R., and Talebizadehsardari, P. (2019). Energetic-exergetic Analysis of an Air Handling Unit to Reduce Energy Consumption by a Novel Creative Idea. *Int. J. Numer. Methods Heat Fluid Flow* 29 (10), 3959–3975. doi:10.1108/HFF-09-2018-0524

Zheng, Y., Kalbasi, R., Karimipour, A., Liu, P., and Bach, Q.-V. (2020). Introducing a Novel Air Handling Unit Based on Focusing on Turbulent Exhaust Air Energy-Exergy Recovery Potential. *J. Energ. Resour. Techn.* 142, 1–10. doi:10.1115/1.4047255

Conflict of Interest: The author declares that the research was conducted in the absence of any commercial or financial relationships that could be construed as a potential conflict of interest.